2004 8th International Conference on
Control, Automation, Robotics and Vision
Kunming, China, 6-9th December 2004

Kinematics Modeling and System Errors Analysis for An AFM Based Nano Manipulator

Xiaojun Tian[1,4] **Ning Xi**[1,2] **Yuechao Wang**[1] **Zaili Dong**[1] **Wenjung Li**[1,3]

1 Shenyang Institute of Automation, Academy of Sciences, Shenyang 110016, China
2 Department of Electrical and Computer Engineering, Michigan State University, East Lansing, MI 48824, USA
3 Department of Automation and Computer-Aided Engineering, CUHK, Hong Kong, China
4 Graduate School, Academy of Sciences, Beijing 100039, China
Email: xjtian@sia.cn

Abstract

During imaging and nanomanipulation with a sample-scanning AFM based nano manipulator, because of bend motion of tube scanner, two important errors will be generated, namely scanning size error and cross coupling error, and they are destructive to both image quantitative analysis and nanomanipulation accuracy. To minimize the errors, a kinematics model of the scanner is presented, which shows that lateral and vertical displacements at any point on sample depend on its offset to tube axis, applied voltage and sample thickness besides scanner geometric parameters and piezoelectric constant. According to the model, the two errors are quantitatively analyzed. Imaging and nanolithography experiments verify the kinematics model and errors calculation formulas, and some methods are also proposed for minimizing the errors.

1 Introduction

Since the invention of atomic force microscope (AFM) by G Binnig in 1986 [1], it has been a standard tool for imaging sample on nanometer scale. Recently it has not only been used in imaging sample, it has been used in nanomanipulation [2][3][4]. Generally AFM includes sample-scanning mode AFM, which means scanner actuates sample moving while probe keeps still, and tip-scanning mode AFM, vise versa. Single Tube scanner is generally used in AFM [5], common structure of single tube scanner in sample scanning AFM is shown in Fig. 1.

The main part of tube scanner is a piezoceramics tube with one end attached to sample stage and the other end fixed on a base. The inside and outside of the tube are plated with metal, and the outside is quartered with two opposite electrodes used as one part. When ambi-polar voltage is applied, the tube will

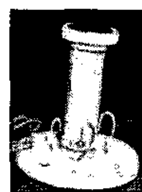

Fig.1. Tube scanner in sample scanning AFM

bend to realize lateral scanning displacement [5]. When voltage is applied to the inside, the vertical displacement will be realized.

During imaging and nanomanipulation with an sample -scanning AFM based nano manipulator, two important errors, namely cross coupling error and scanning size error, will be generated due to bend motion of tube scanner, and the two errors are destructive to both image and probe positioning accuracy in nanomanipulation. Many researches have been done on tube scanner errors caused by piezoceramics intrinsic characteristics such as nonlinearity and hysterisis, and many calibration and nonlinearity correction methods have also been proposed [6][7][8][9]. Some models mainly to investigate scanner dynamics have also been proposed, e.g., a complex dynamic model considering the coupling between motions in different axes has been presented [10], and a linear fifth-order model of the scanner lateral dynamics for open-loop control to enable fast imaging has been investigated [11]. While system errors quantitative analysis, to which kinematics modeling is indispensable, has seldom been done.

In this paper, kinematics model of tube scanner is presented based on its motion analysis. And scanning size error and cross coupling error according to the model are quantitatively analyzed, which shows that scanning size error is greatly affected by sample thickness and nominal scanning size, while vertical cross coupling error is

0-7803-8653-1/04/$20.00 © 2004 IEEE

greatly affected by probe tip offset to tube axis and nominal scanning size. Imaging and nanolithography experimental results have verified the proposed model and errors calculation formulas.

2 Kinematics Model of Tube Scanner

When ambi-polar voltage is applied on two opposite electrodes of scanner outside, the tube will bend as shown in Fig.2, and sample will generate lateral translation and rotation relative to fixed probe, thus displacement of any point on sample is different.

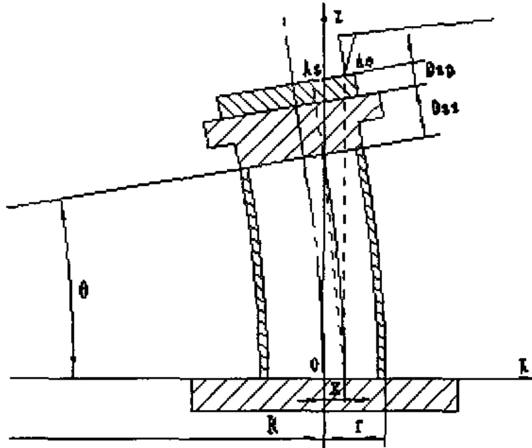

Fig.2. Kinematics model of single tube scanner of sample-scanning AFM

In Fig.2, the part clipped by angle θ is piezoceramics tube, the part pointed by Dss is sample stage, and Dsp means sample.

If material of scanner is uniform and structure is symmetric, and scanner axis is viewed as symmetric axis, the extension and condensation will be the same with ambipolar voltage applied to two opposite electrodes, and the bend geometry can be viewed as circular arc [12], then we have

$$\begin{cases}(R+r)\theta=L+\Delta L \\ (R-r)\theta=L-\Delta L\end{cases} \quad (1)$$

Where r is the outside radius of tube, R is the curvature radius of the tube axis, θ is the central angle, L is the initial length of tube, and ΔL is the extension of tube after voltage U_x is applied to the tube.

The extension of tube can be presented [13] as

$$\Delta L = Ed_{31}L = \frac{d_{31}L}{t}U_x \quad (2)$$

Where E is the electric field intensity along tube wall, U_x is voltage along x axis, t is thickness of tube wall, and d_{31} is piezoelectric constant along tube axis.

Submitting equation (2) into (1), one can obtain the expression of θ

$$\theta = \frac{L}{R} = \frac{d_{31}L}{tr}U_x \quad (3)$$

Before tube bends, the lateral coordinate of any point on sample is x, and vertical coordinate is $L + Dss + Dsp$. After tube bends to left as shown in Fig.2, the point moves to point As, then the displacement of the scanner (any point on sample) can be presented as

$$dx = (R+x)(1-\cos\theta) + (Dss+Dsp)\sin\theta \quad (4)$$

$$dz = ((R+x)\sin\theta - L) + (Dss+Dsp)(\cos\theta - 1) \quad (5)$$

When tube extends, tube wall thickness will reduce and the change will be $\Delta t = d_{33}U_x$ [13], Where d_{33} is piezoelectric constant vertical to tube axis. For d_{33} is on sub-nanometer per voltage scale [13], and generally U_x is below one thousand voltages, Δt is on sub-micrometer scale and compared with t on millimeter scale, Δt can be ignored and t can be viewed as a constant.

Thus for t, r, L and d_{31} are all constants for a given scanner, θ and R only depend on U_x according to equation (3), and Dss is also a constant, the lateral and vertical displacements dx and dz at any point on sample depend on applied voltage (U_x), its offset to tube axis (x) and sample thickness (Dsp).

3 Scanning Size Error and Cross Coupling Error

As shown in Fig.2, the lateral position of probe tip contacting the point, corresponding to the center of scanning area on sample, is decided by its offset to scanner axis, which can be adjusted manually by adjusting tube scanner base position before imaging starts.

After tube bending shown in Fig.2, the sample's point touched by probe tip has changed from point As to point Ae as shown in Fig. 2, and point Ae's vertical coordinate z_{Ae} is

$$Z_{Ae} = (R+x)\tan\theta + (Dss+Dsp)/\cos\theta \quad (6)$$

Thus the right scanning area covers the area from point Ae to point As, and its size can be obtained as

$$Lrss = [(R+x)(1-\cos\theta) + (Dss+Dsp)\sin\theta]/\cos\theta \quad (7)$$

Likewise, when tube bends right, the size of left scanning area $Llss$ can also be obtained according to the method mentioned above

$$Llss=[(R-x)(1-\cos\theta)+(Dss+Dsp)\sin\theta]/\cos\theta \quad (8)$$

Then the whole scanning size Lss with tube bending to left and right can be deduced from Eqs (7) and (8)

$$Lss=2[R(1-\cos\theta)+(Dss+Dsp)\sin\theta]/\cos\theta \quad (9)$$

With parameters analyzed in section 2, the scanning size Lss depends on U_x and Dsp.

3.1 Scanning Size Error

AFM is calibrated before sample scanning, the thickness of the grating used in lateral calibration can be called nominal sample thickness $Dnsp$, after calibration scanning size can be called nominal scanning size $Lnss$, which is a pointed value on the scanning program interface and can be easily changed by user, and it can be obtained from equation (9) as

$$Lnss=2[R(1-\cos\theta)+(Dss+Dnsp)\sin\theta]/\cos\theta \quad (10)$$

For $Dnsp$ is a constant and θ and R only depend on U_x, $Lnss$ also only depends on U_x, which means that $Lnss$ is corresponding to θ or R.

When sample thickness is not equal to nominal one, there will be an error between actual scanning size and nominal one. From Eqs (9) and (10), scanning size error $dLss$ can be presented as

$$dLss=2(Dsp-Dnsp)\tan(\theta) \quad (11)$$

For $Dnsp$ is a constant, $dLss$ depends on Dsp and θ that corresponds to $Lnss$, and the simulation result of scanning size error $dLss$ dependence on sample thickness Dsp and nominal scanning size $Lnss$ is shown in Fig. 3.

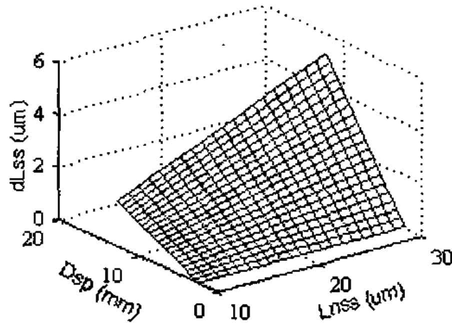

Fig3. Simulated dependent curve of scanning size error on sample thickness and nominal scanning size (while nominal sample thickness is 2mm with tube length 52mm and sample stage thickness 4mm)

3.2 Cross Coupling Error

3.2.1 Vertical Cross Coupling Error Caused by Lateral Displacement

After tube bend to left shown in figure 2, the vertical cross coupling error dZr deduced from equation (6) is

$$dZr=[(R+x)\tan\theta-L]+[(Dss+Dsp)(1/\cos\theta-1)] \quad (12)$$

With parameters analyzed in section 2, it can be seen that vertical cross-coupling error depends on its offset (also probe tip offset) to tube axis, nominal scanning size and sample thickness and the simulation result is shown in Fig. 4.

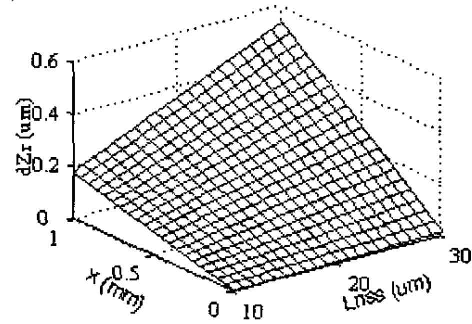

Fig. 4. Simulated dependent curve of vertical cross coupling error on tip offset to tube axes and nominal scanning size (while sample thickness keeps 2mm with tube length 52mm and sample stage thickness 4mm)

Specially, when the point's offset to tube axis is zero and sample thickness is equal to nominal one, the simulated result of vertical cross coupling error dependence on scanning size is show in Fig. 5.

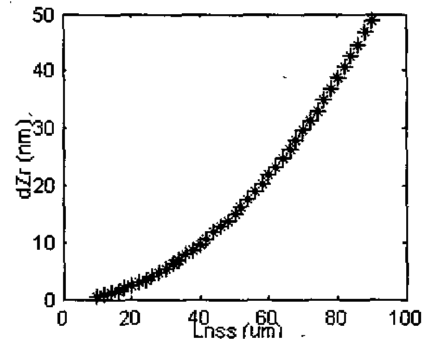

Fig5. Simulated dependent curve of vertical cross coupling error on scanning size with offset equal to zero (while sample thickness is 2mm with tube length 52mm and sample stage thickness 4mm)

It can be seen that the error in Fig. 5. is very small compared with that in Fig. 4. especially when scanning size is small, which means that the offset is a dominant factor causing vertical cross coupling error.

3.2.2 Lateral Cross Coupling Error Caused by Vertical Displacement

If additional voltage Uz is applied to the inside of the tube while tube is bending, an additional lateral error will be caused. At that time, the additional extension of tube can be presented as

$$\Delta Lz = \frac{d_{31}L}{t}U_z \tag{13}$$

And the additional lateral error is

$$\Delta Xzc = \Delta Lz \sin\theta \tag{14}$$

For the maximal value ΔLz caused by Uz is only a few micrometers and the maximal central angle is below 0.001 radian in experiments, then ΔXzc is on sub-nanometer scale and can be ignored.

4 Experiment and Verification

In order to verify the proposed model and error calculation formula, some imaging of gratings and nano lithography are performed.

4.1 System Configuration

A CSPM-2000wet AFM (Ben Yuan Ltd., China) was used for imaging and nanomanipulation. A scanner is equipped in the AFM head with a maximum XY scan range of 30um X 30um and a Z range of 3um. Silicon nano-probe (MickoMasch Inc.) with V-shaped cantilevers is used. In order to facilitate imaging and nanomanipulation, an optical microscope and a CCD camera are also included in system shown in Fig. 6.

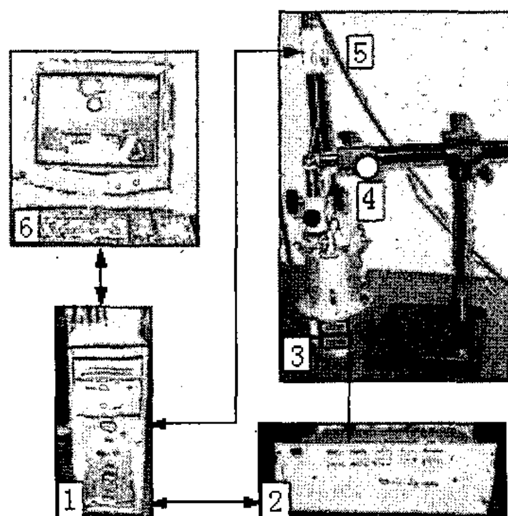

Fig. 6. The configuration of AFM based imaging and nanomanipulation system: 1, AFM control computer; 2, CSPM 2000wet controller; 3, AFM head; 4, optical microscope; 5, CCD camera; 6, monitor

In the system, the AFM head is controlled by CSPM 2000wet controller connected to computer. The computer responds for running system control program and provides an interface for user. The optical microscope and CCD camera help the operator to adjust the laser to focus on cantilever end and search for interesting area on sample.

4.2 Scanning Size Error and Analysis

To grating with 3 um width's steps (MickoMash Inc.), actual scanning size rises with grating thickness increasing as shown in Fig. 7.

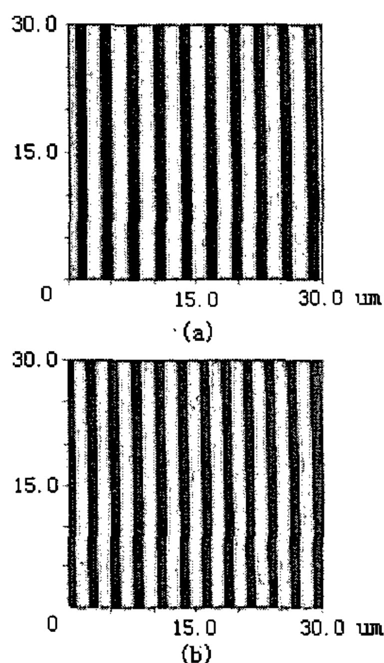

Fig. 7. Two scanning images of grating with grating thickness 2mm (a) and 10mm (b) while nominal scanning size keeps 30um

Adjusting grating thickness, we can get the change table of scanning size as shown in table 1.

Sample thickness/mm	Measured scanning size/um	Theoretical scanning size/um
2	30.0	30.000
4	31.0	31.034
6	31.9	32.068
8	33.2	33.103
10	34.1	34.137

Table 1. Measured scanning size and theoretical one with sample thickness changing (nominal scanning size keeps 30um)

From experiments we can conclude that experimental data is accordant with theoretical one. When sample thickness

equals to nominal one, actual scanning size is equal to nominal one. While if the two ones are not the same, actual scanning size will be greatly affected by sample thickness and nominal one. Keeping nominal scanning size constant, the actual one will increase with sample thickness increasing. So for minimizing scanning size error, we can firstly increase or decrease sample thickness to make it equal to nominal one. To special sample whose thickness cannot be changed, we can compensate it by equation (11).

4.3 Vertical Cross Coupling Error and Analysis

Before scanning, the sample will actuated to approach to probe tip and tip will touch at a point on sample, and the point corresponding to the center of scanning area is decided by tip offset to scanner axis shown in Fig.2, which can be adjusted manually by adjusting tube scanner base position before imaging starts.

For the height error of the grating steps' top surface is only 1.5nm (Mikromasch Inc.), its surface can be considered as an even plane for measuring vertical cross coupling error shown in Fig. 8.

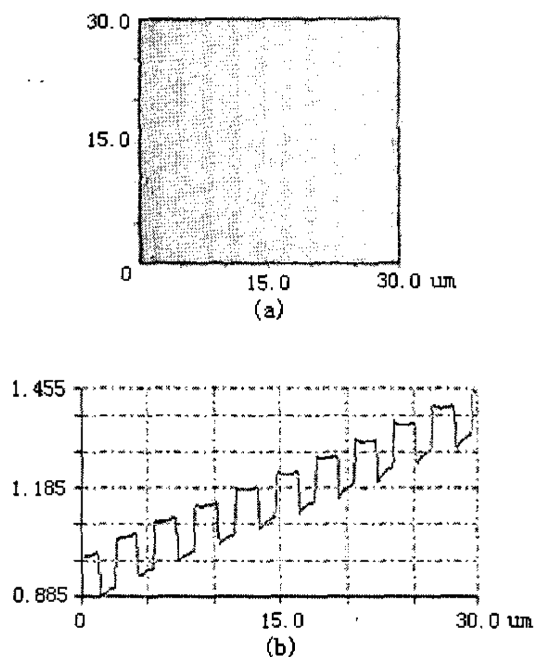

Fig. 8. Scanning image (a) and its section image (b) of grating with tip offset equal to 0.5mm when scanning size is 30um (Note that in the cross section image (b), the effect of hysteresis and creep is obvious, while the "bow" shape is not obvious for the effect of bow effect in vertical direction is very small compared with the effect caused by the tip offset, especially when the scanning size is small.)

Changing tip offset when nominal scanning size keeps 30um, we get the table of vertical cross coupling error changing as shown in table 2.

Tip offset /mm	Measured vertical cross coupling error /nm	Theoretical vertical cross coupling error /nm
-0.5	-261	-253
-0.25	-119	-124
0	9	5
+0.25	130	134
+0.5	250	263

Table 2. Vertical cross coupling error with tip offset changing from -0.5mm to 0.5mm(nominal scanning size keeps 30um)

Thus we can conclude that experimental data is accordant with theoretical one. When tip offset is zero and scanning size is small, vertical cross coupling error is small. While tip offset is not zero, vertical cross coupling error will rise greatly with tip offset increasing.

Although vertical cross coupling error in imaging caused by tip offset can be minimized by post-imaging correction method, it still exists in nano lithography as shown in Fig. 9.

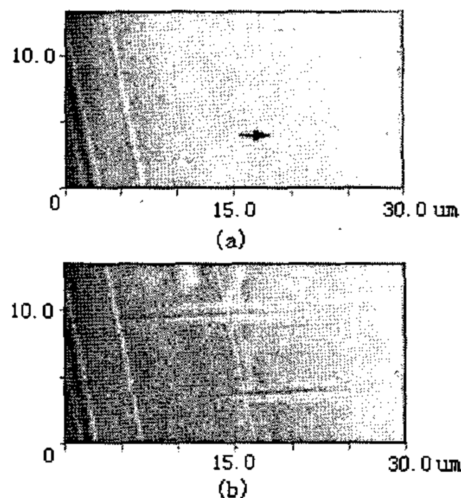

Fig. 9. Scanning images of polycarbonate before lithography (a) and after lithography (b) at the two lithography lines while tip locates on the right of tube axis. The slim line-like particle pointed by arrow in left image is pushed aside by tip with force feedback off in image (b), where the set-point value at the above deeper lithography line is larger than that of the below line

In image (a) of Fig. 9., although the sample has been adjusted horizontal before scanning, we can still see that the right side of sample moves higher than the left for tip locates at the right of tube axis with tip offset being 1mm. And especially in image (b) of Fig. 9., we can see that the lithography line becomes

deeper from left to right, which also has the same meaning as that in image (a) and validates the model proposed above. So for minimizing vertical cross coupling error in nanomanipulation, tip offset to tube axis can be firstly reduced to zero by adjusting the lateral position of tube scanner base, while for those occasion where tip offset can't be adjusted to zero, we can compensate it in trajectory planning of nanomanipulation according to error calculation formula shown as equation (12).

5 Conclusion

Scanning size error and cross coupling error greatly affect the accuracy of imaging and nanomanipulation for sample-scanning AFM based nano manipulator. With scanning size error and cross coupling errors quantitatively analyzed according to the kinematics model presented in this paper, some methods mentioned above can be adopted to minimize the errors, thus the accuracy in scanning and manipulation can be greatly enhanced.

Acknowledgment

This research work is supported under NHTRDP (863 program) Grants 2002AA422210 and here we also thank for the support and help from Ben Yuan Ltd. and Mr. Junhan Wu .

Reference

[1] G. Binnig, C. F. Quate, and C. Gerber, "Atomic force microscope", *Physical Review Letters*, vol. 56, no. 9, pp. 930-933, 1986,.

[2] R. Luthi, E. Meyer, H. Haefke, L. Howald, W. Gutmannsbauer, and H.-J. Guntherodt, "Sledtype motion on the nanometer scale: Determination of dissipation and cohesive energies of c60", *Science*, vol. 266, pp. 1979-1981, 1994.

[3] D. M. Schaefer, R. Reifenberger, A. Patil, and R. P. Andres, "Fabrication of two-dimensional arrays of nanometer-size clusters with the atomic force microscope", *Applied Physics Letters*, vol. 66, pp. 1012-1014, 1995.

[4] T. Junno, K. Deppert, L. Montelius, and L. Samuelson, "Controlled manipulation of nanoparticles with an atomic force microscope", *Applied Physics Letters*, vol. 66, no. 26, pp. 3627-3629, 1995.

[5] G. Binnig and D. P. E. Smith, "Single-tube three-dimensional scanner for scanning tunneling microscopy", *Review of Scientific Instruments*, vol. 57, no. 8, pp. 1688-1689,1986.

[6] J. F. Jørgensen, L. L. Madsen, J. Garnaes, K. Carneiro, K. Schaumburg, "Calibration, drift elimination and molecular structure analysis", *Journal of Vacuum Science and Technology*, vol. B12, no. 3, pp. 1698-1701, 1994.

[7] R. Durselen, U. Grunewald, W. Preuss, "Calibration and applications of a high-precision piezo scanner for nanometrology", *Journal of Scanning Microscopies*, vol. 17, no. 2, pp. 91-96, 1995.

[8] S. Ito, "Linearity correction systems for the image distortion in atomic force microscope", in *Proceedings of the SICE Annual Conference*, pp. 927-930, 1994.

[9] J. Akila, S. S. Wadhwa, "Correction for nonlinear behavior of piezoelectric tube scanners used in scanning tunneling and atomic force microscopy", *Review of Scientific Instruments*, vol. 66, no. 3, pp. 2517, 1995.

[10] O. M. El Rifai, K. Youcef-Toumi, "Coupling in piezoelectric tube scanners used in scanning probe microscopes", in *Proceedings of the American Control Conference*, vol. 4, pp. 3251-3255, 2001.

[11] G. Schitter, A. Stemmer, "Model based signal conditioning for high-speed atomic force and friction force microscopy", *Microelectronic Engineering*, vol. 67-68, pp. 938-944, June, 2003,

[12] C. Wei, H. H. Zhang, L. Tao, W. J. Li, and H. M. Shi, "A circular arc bending model of piezoelectric tube scanners", *Review of Scientific Instruments*, vol. 67, no. 6, pp. 2286, 1996.

[13] J. A. Gallego-Juarez, "Piezoelectric ceramics and ultrasonic transducers", *Journal of Physics E: Scientific Instruments*, vol. 22, pp. 804-816, 1989.